We are IntechOpen,
the world's leading publisher of
Open Access books
Built by scientists, for scientists

6,900
Open access books available

185,000
International authors and editors

200M
Downloads

154
Countries delivered to

Our authors are among the

TOP 1%
most cited scientists

12.2%
Contributors from top 500 universities

CLARIVATE ANALYTICS
BOOK CITATION INDEX
INDEXED

WEB OF SCIENCE™

Selection of our books indexed in the Book Citation Index
in Web of Science™ Core Collection (BKCI)

Interested in publishing with us?
Contact book.department@intechopen.com

Numbers displayed above are based on latest data collected.
For more information visit www.intechopen.com

Control of Redundant Submarine Robot Arms under Holonomic Constraints

E. Olguín-Díaz, V. Parra-Vega and D. Navarro-Alarcón
Robotics and Advanced Manufacturing Division
Research Center for Advanced Studies-CINVESTAV
Saltillo, México

1. Introduction

AUV has undergone a major leap as technology allows higher integration, while faster sensors and actuators and new modelling techniques and its corresponding control algorithms are available. One of the new improvements of AUV technology is the capability to produce dexterous motion using robot manipulators as its end effector. This robot manipulator behaves as a multi-degrees of freedom active tool, such that the AUV stands as the free-floating base of the robot manipulator. In this case, the AUV navigates to drive the RA to its working environment, with two independent controllers, one for the AUV and another one for the RA. However, when the RA is working out its task, it is convenient to automatically control the whole AUV+RA, coined in this paper as Submarine Robot Arm or SRA for short, as a whole and unique system so as to take advantage of its redundancy and achieve better accomplishment in comparison to control the AUV and the RA independently.

When the RA is in contact to a rigid object, a constrained SRA appears and the control system now must control additionally the contact forces. This sort of systems have become a new area in AUV technologies, however there is no available and proved control system for constrained SRA, which posse a complex problem because there appears a tightly coupled hyper-redundant nonlinear system subject to holonomic constraint, which produces all together a set of nonlinear algebraic differential equations of index 2.

Constrained SRA deals simultaneously with navigation of its non-inertial base while controlling the pose and contact force of its RA. For the general case, we would have a free-floating hyper-redundant constrained RA. Additionally, the holonomic constraint must be satisfied all the time to maintain stable contact to a rigid underwater object, thus an efficient force controller is required to achieve stable contact while exerting a given desired contact force on this object. This rather new problem deserves a separate attention in AUV technologies, due to the subtle complexities of constrained SRA in its own right.

1.1 Contribution

After a brief discussion in Section 2 on the nature of the control problem of constrained SRA, which deserves a particular treatment apart to the AUVs control problem, we go through the full dynamic model of an SRA in Section 3. Then, Section 4 shows the key design of the

open-loop error system. In Section 5 a quite simple force/posture model-free decentralized control structure is proposed, which guarantees robust tracking of time-varying contact force and posture, without any knowledge of SRA dynamics, which manage redundancy to introduce primary and secondary tasks. Closed-loop stability properties are obtained in the sense of Lyapunov and Variable Structure Systems arguments deliver second order sliding modes to obtain very fast tracking, while satisfying both tasks. A representative set of simulations for a 12 DoF SRA system are presented and discussed in Section 6. Some remarks are presented in Section 7, and final conclusions are given in Section 8.

2. The motion control problem of redundant constrained SRA

Controlling redundant constrained SRA subject to holonomic constraints requires the latest scientific knowledge and technological achievements for AUV and RA, from a simple torpedo to modern AUV and RA subject to hydrodynamic forces. Those vehicles pose at the same time tantamount scientific and technological challenges in robotics, control, man-machine interfaces, submarine telecommunications and mechatronics. This kind of SRA systems provide dexterity to a level yet unknown in AUV, which some day could superpose the limited capabilities of deep water divers, where bulky equipment is required to survive, thus less dexterity is exhibited at this waters by human divers. Despite these evident benefits, little study has been published on the automatic control of this systems. So far, must of the contributions point out on how to provide an acceptable level of (perhaps autonomous or automatic) navigation capabilities of the main body of the AUV, without compromising security, rather than in the manipulation capabilities of its tools, perhaps a RA with few DoF. Therefore, we bring the attention of a new breed of AUV whose main task is manipulation, perhaps with more than one robot arm, where the underlined issue is that the main body, the AUV, is considered as a free-floating fully actuated base. Notice that a common assumptions on this problem is that AUV is several times heavier than the RA so as to provide inertial decoupling between the AUV and the robot arm. For this case, the control system is designed so as to controlling independently the base and the arm, while a coupling endogenous disturbance is presented. In this case, we have n trusters to drive the AUV and m actuators to drive the SRA. However, with lighter materials and batteries and powerful trusters, this assumption may fail, since the mass and inertial might be quite similar and singular perturbation theory hardly applies anymore. As a consequence, technological improvements bring coupling and thus more elaborated control schemes are required to deal with the whole nonlinear highly coupled dynamics, from the base AUV to the end-effector RA, as one integrated free-floating constrained system.

2.1 The free-motion SRA problem
Pioneering efforts on SRA were focused on motion control with simple PD regulators in unconstrained (free-motion) motion, similar to the case of fixed-base robots in our labs. Acceptable performance for tracking has been proposed using more complicated (saturated or nonlinear) PID schemes and few model-based controllers have been proposed for tracking, under lab conditions (Spong; Villani et al.). In (Smallwood & Whitcomb), some heuristical simplifications are propose to deal with simple control techniques, however formal results are not provided, which may become potentially unstable under several possible working conditions. Though the Euler Lagrange dynamics, coming from the

Kirchhoff formulation and its equivalence in Euler-Lagrange formalisms shows passivity and nice energetic properties, and although it seems plausible that several passivity-based techniques could be extended to the realm of SRA, few publications address this problem in comparison to the wide variety of available passivity-based techniques for fixed-based RA. Automatic unconstrained motion control problem of SRA, though formally studied during the last two decades, is still in its infancy basically due to the fact that the full nonlinear model is quite complex, besides that the estimation of physical parameters are really difficult to obtain, so model-based controllers are difficult to implement. This is one reason why human operators are still the preferred controllers at risky missions. Since the model is hardly available, soft-computing techniques may be an option to approximate the inverse dynamics and implement controllers with implicit knowledge of the full system, however, no formal publications are known by the authors in this area for the full nonlinear model with formal stability results.

When the task is to achieve contact between the end-effector and a rigid object clamped on the sea floor or in a submarine structure, contact wrenches are propagated all over the RA and along the AUV through its rigid structure. Powerful and quick trusters are required to establishing, maintain and achieve stable contact, and finally to exert forces while moving along the surface of the object. This is known as the constrained SRA problem.

2.2 The constrained SRA problem

Stable contact for SRA is a more complex problem in comparison to the typical force/position control problem of robot manipulators fixed to ground in our laboratory because not only complementary complex dynamics are presented in SRA, such as buoyancy and added masses, as well as complex hydrodynamic effects, but to the fact that the vehicle reference frame is not longer inertial, see (Schjølberg & Fossenl; E. Olguín Díaz), thus there is not a fixed reaction point to react to. Thus, in this case, the truster of the AUV must react accordingly to hold still or accommodate these forces while still achieving simultaneously tracking not only for the UAV but also for the RA.

However, more interesting submarine tasks involves the more challenging problem of establishing stable contact while moving along the contact surface, like pushing itself against a wall or polishing a sunken surface vessel surface or manipulating tools on submarine pipe lines. In all these cases, contact forces are presented, and little is known about the structural properties of these contact forces, let alone exploit them either for design or control. This problem leads us to study the simultaneous force and pose (position and orientation) control of free-floating SRA under realistic conditions. By realistic we mean that the full nonlinear coupled dynamics are considered subject to holonomic constrains.

In the sequel, we assume that the dynamical model, and its parameters, are hardly known in practice, though the the full state is available as well as the geometric description of the contact surface or object.

There are two main general reasons that help us to explain why that force/posture problem remains rather an open problem. One reason is that we really know little about how to exploit its apparent generously well-behaved and slow dynamics. On one hand, how to model and control properly a fully immersed vehicle with a RA constrained by rigid object is an open issue in terms of exploitation of its passivity properties, when the model is subject to holonomic constrains. The second reason is rather technological and economical. On one hand, present day commercial submarine force control technology lies behind today system

requirements, such as very fast sampling and uniform rates of sensors and actuators, as well as low power consumption, even when the bandwidth of the submarine robot is very low.

Despite brilliant -for the simplicity of this complex problem- control schemes for free motion submarine robots published in the past few years, in particular those of (Yoerger & Slotine; Smallwood & Whitcomb 2001; Smallwood & Whitcomb 2004) does not formally guarantee convergence of tracking errors, let alone simultaneous convergence of posture and contac force tracking errors. There are several results that suggest empirically that a simple PD control structure behaves as stiffness control for submarine robots to produce acceptable low performance contact tasks. However, for more precise and fast tasks, the fast simultaneous convergence of timevarying contact forces and posture remains an open problem.

Since SRA dynamics are very hard to known exactly in practice, the dynamic model and its dynamic parameters should be considered uncertain, or at least parametrically unknown. Recently, some efforts have focused on how to obtain simple control structures to control the time-varying pose of the AUV under the assumption that the relative velocities are low (Smallwood & Whitcomb 2004; Perrier & Canudas de Wit). For force control of SRA, when dynamics are unknown, virtually none complete and formal control system is known. We believe that to obtain better performance in contact tasks a better understanding of the structural properties of submarine robots in stable contact to rigid objects are required. To this end, we assume that the rigid body dynamics of SRA is subject the now well-known holonomic constraints and thus we can extend some schemes to the case of SRA. Notice that during rigid contact the system exhibits similar structural properties of fixed-base constrained robots, under the full formulation of the Kirchhoff dynamics. Thus, in this paper we have chosen the Orthogonalization Principle (Parra-Vega & Arimoto) to extend from fix base to free-floating base to redundant SRA to propose a simple, yet high performance, controller with advanced tracking stability properties.

2.3 The constrained redundant SRA problem

When the SRA is redundant, there is some degrees of freedom available that can be used to satisfy a secondary task, being the primary task convergence of tracking errors. For instance, the AUV could be relocated dynamically all over the time at the pose of minimum power consumption such that the RA carries out the main task with greater manipulability index or avoiding joint limits or avoiding obstacles or with less energy consumption or keeping the AUV in a still position while the RA moves around.

If we could pursue primary and secondary tasks fulfillment, then some sort of Cost Index should be penalized, similar to the case of free motion grounded robots. That is, the cost function may constraint the motion of the SRA's base within an envelope to achieve better manipulability index or to minimize control effort/energy without compromising maneuverability, while tracking desired force/posture trajectories. In any case, besides the simultaneous tracking control problem of position and force, for redundant SRA, an optimal control problem is involved, which could be treated at the kinematic or dynamic level to take full advantage of the capability to carry out simultaneously a primary and secondary task. In this way, a certain degree of dexterity can be introduced when solving online the redundancy of the SRA.

3. The full nonlinear coupled model of the SRA

For completness, the AUV dynamic model is presented firstly, including under contact. That is a six DOF AUV is derived, including contact wrench. Then, the RA is attached to the AUV to build the SRA and the full expresions are presented.

3.1 The AUV model

The model of a submarine can be obtained with the momentum conservation theory and Newton's second law for rigid objects in free space via the Kirchhoff formulation (Fossen), the inclusion of hydrodynamic effects such as added mass, friction and buoyancy and the account of external forces/torques like contact effects (Olguín Díaz). The model is then expressed by the next set of equations:

$$M_v\dot{v}_v + C_v(v_v)v_v + D_v(v_v,t)v_v + g(q_v) = u_v + F_c^{(v)} + \eta_v(v_v,t), \tag{1}$$

$$v_v = J_v(q_v)\dot{q}_v \tag{2}$$

From this set, (1) is called the dynamic equation while (2) is called the kinematic equation. The generalized coordinates vector $q_v \in \Re^6$ is given on one hand by the 3D Cartesian position $d_v = (x_v, y_v, z_v)^T$ of the origin of the submarine frame (Σ_v) with respect to a inertial frame (Σ_0), and on the other hand by any set of attitude parameters that represent the rotation of the vehicle's frame with respect to the inertial one. Most common sets of attitude representation such a Euler angles, in particular roll-pitch-yaw (ϕ, θ, ψ), use only 3 variables (which is the minimal number of orientation variables). Then, for a submarine, the generalized coordinates represents its 6 degrees of freedom:

$$q_v = \begin{pmatrix} d_v \\ \vartheta_v \end{pmatrix} \tag{3}$$

where $\vartheta_v = (\phi_v, \theta_v, \psi_v)^T$ stands for the attitude parameter vector.

The vehicle velocity $\nu_v \in \Re^6$ is the velocity wrench (vector representing both linear and angular velocity) of the submarine in the vehicle's frame. This vector is then defined as $v_v = (v_v^{(v)T}, \omega_v^{(v)T})^T$ The relationship between this vector and the generalized coordinates is given by the kinematic equation. The linear operator $J_v(q) \in \Re^{6 \times 6}$ in (2), is built by the concatenation of two transformations. The first is $J_q(q_v) \in \Re^{6 \times 6}$ which converts time derivatives of generalized coordinates to velocity wrench in the inertial frame. This operator is necessary because the angular velocity of a body (ω) is not given by the time derivative of its angular parameters $(\dot{\vartheta} \neq \omega)$. However, there is always a transformation operator given by the very specific type of chosen orientation parameters:

$$\omega_v = J_\theta(\vartheta)\dot{\vartheta}_v \tag{4}$$

Then the operator $J_q(q_v)$ is defined as:

$$J_q(q_v) \triangleq \begin{bmatrix} I & 0 \\ 0 & J_\theta(q_v) \end{bmatrix} \tag{5}$$

The second operator is

$$J_{R_v}(q_v) = \begin{bmatrix} R_0^v & 0 \\ 0 & R_0^v \end{bmatrix} \in \Re^{6 \times 6} \tag{6}$$

which transforms a 6 dimension tensor from the inertial frame to vehicle's frame. The matrix $R_0^v (\vartheta_v) \in SO_3$ is the rotation matrix of the vehicle. Thus, the linear operator is defined as

$$J_\nu(q) \stackrel{\triangle}{=} J_R^T(q) J_q(q)$$

A detailed discussion on the terms of (1) can be found in (Olguín Díaz & Parra-Vega).

In the dynamic equation (1), matrices $M_v, C_v(\nu), D_v(\cdot) \in \Re^{6 \times 6}$ are Inertia matrix, Coriolis matrix and Damping matrix. M_v includes the terms of classical inertia plus the hydrodynamic coefficients of the added mass effect (due to the amount of extra energy needed to displace the surrounding water when the submarine is moving). The Inertia matrix is constant, definite positive and symmetric only when the submarine is complete immersed and the relative water incidence velocity is small (Fossen). This condition is met for a great amounts of activities. The Coriolis vector $C_v(\nu)\nu$ represents the Coriolis and gyroscopic terms, plus the velocity quadratic terms induced by the added mass. The Coriolis matrix in this representation does not depend on the position but only on the velocity, in contrast to the same expression for a Robot Manipulator. It is indeed skew symmetric and fulfills the classic relationship for Lagrangian systems: $\dot{M}_v - 2C_v(\nu) = Q; Q+Q^T = 0$. The Damping matrix represents all the hydrodynamic effects of energy dissipation. For that reason it is a strictly positive definite matrix, $D_v(q, \nu, t) > 0$. Its arguments are commonly the vehicle's orientation ϑ_v, the generalized velocity ν, and the velocity of the surrounding water $\zeta(t)$. The diagonal components represents the drag forces while the off-diagonal components represent the lift forces. Vectors $g_v(q)$, u, $F_c^{(v)} \in \Re^6$ are all force wrenches (force-torque vector) in the vehicle's frame. They represent respectively: gravity, input control and the contact force. Gravity vector includes buoyancy effects and it does not depend on velocity but on the orientation (attitude) of the submarine with respect to the inertial frame. The contact force wrench is the one applied by the environment *to* the submarine. The input control are the forces/torques induced by the submarine thrusters in the vehicle frame.

The disturbance $\eta_v (\nu, \zeta(t), \dot{\zeta}(t))$ of the surrounding fluid depends mainly in the incidence velocity, i.e. the relative velocity of the vehicle velocity and the fluid velocity. The last is a non-autonomous function, but an external perturbation. This disturbance has the property of

$$\eta_v (\nu, 0, 0) = 0. \tag{7}$$

That is that all the disturbances are null when the fluid velocity and acceleration are null.

The dynamic model (1)-(2) can be rearranged by replacing (2) and its time derivative into (1). The result is one single equation model:

$$M_q(q_v)\ddot{q}_v + C_q(q_v, \dot{q}_v)\dot{q}_v + D_q(\cdot)\dot{q}_v + g_q(q_v) = u_{q_v} + \tau_c + \eta_q(\dot{q}_v, \zeta(t), \dot{\zeta}(t)); \tag{8}$$

which, whenever $\zeta(t) = \dot{\zeta}(t) = 0$, i.e. $\eta_q(\cdot) = 0$, has the form of any Lagrangian system. Its components fulfills all properties of such systems i.e. definite positiveness of inertia and damping matrices, skew symmetry of Coriolis matrix and appropriate bound of all components (Sagatun & Fossen). The control input in this equation is obtained by a linear transformation of the real input using the linear operator given by the kinematic equation:

$$u_{q_v} = J_\nu^T(q_v) u_v \tag{9}$$

The contact effect is also obtained by the same transformation. However it can be expressed directly from the contact wrench in the inertial frame (Σ_0) by the relationship

$$\tau_c = J_\nu^T(q_v) F_c^{(v)} = J_q^T(q_v) F_c^{(0)}, \tag{10}$$

where the contact force $F_c^{(0)}$ is the one expressed in the inertial frame. By simplicity it will be noted as F_c from this point further. The relationship with the one expressed in the vehicle's frame is given by $F_c = J_R^T(q) F_c^{(v)}$. This wrench represents the contact forces/torques exerted by the environment to the submarine as if measured in a non moving frame. These forces/torques are given by the normal force of an holonomic constraint when in contact and the friction due to the same contact. For simplicity in this work, tangential friction is not considered. The equivalent of the disturbance is obtained also with the linear operator given as:

$$\eta_q(\cdot) = J_\nu^T(q) \eta_v(\cdot). \tag{11}$$

3.2 Contact force due to an holonomic constraint

A holonomic constraint (or infinitely rigid contact object) can be expressed as a function of the generalized coordinates of the submarine as

$$\varphi(q_v) = 0, \tag{12}$$

with $\varphi(q_v) \in \Re^r$, where r stands for the number of independent contact points between the SRA and the motionless rigid object. Equation (12) means that stable contact appears while the SRA submarine does not deattach from the object $\varphi(q_v) = 0$. Evidently all time derivatives of (12) are zero, which for $r = 1$

$$J_\varphi(q_v) \dot{q}_v = 0 \tag{13}$$

where $J_\varphi(q_v) = \dfrac{\partial \varphi(q_v)}{\partial q_v} \in \Re^{r \times 6}$ is the constraint jacobian. Last equation means that velocities of the submarine in the directions of constraint jacobian are restricted to be zero. This directions are then normal to the constraint surface $\varphi(q_v)$ at the contact point. As a consequence, the normal component of the contact force has exactly the same direction as those defined by $J_\varphi(q_v)$, consequently, the contact force wrench can be expressed as

$$F_c = J_{\varphi+}^T(q_v) \lambda \tag{14}$$

where $J_{\varphi+}(q_v) \equiv \dfrac{J_\varphi}{J_\varphi}$ is a normalized version of the constraint jacobian; $\lambda \in \Re^r$ is the magnitude of the normal contact force at the origin of vehicle frame: $\lambda = \|F_c\|$. The free moving model expressed by (1)-(2), when no fluid disturbance and in contact with the holonomic constraint can be rewritten as:

$$M_v \dot{\nu} + h_v(q_v, \nu, t) \quad = \quad u_v + J_R^T(q_v) J_{\varphi+}^T(q_v) \lambda, \tag{15}$$

$$\nu \quad = \quad J_\nu(q_v) \dot{q}_v, \tag{16}$$

$$\varphi(q_v) \quad = \quad 0, \tag{17}$$

where $h_v(q_v, \nu, t) = C_v(\nu)\nu + D_v(q_v, \nu, t)\nu + g_v(q_v)$. Equivalently, the model (8) is also expressed as

$$M_q(q_v) \ddot{q}_v + h_q(q_v, \dot{q}_v, t) \quad = \quad u_{q_v} + J_{\bar{\varphi}}^T(q_v) \lambda, \tag{18}$$

$$\varphi(q_v) \quad = \quad 0, \tag{19}$$

with $h_q(q_v, \dot{q}_v, t) = C_q(q_v, \dot{q}_v)\dot{q}_v + D_q(q_v, \dot{q}_v, t)\dot{q}_v + g_q(q_v)$ and $J_{\bar{\varphi}}(q_v) = J_{\varphi+}(q_v) J_q(q_v)$. Equations (18)- (19) are a set of Differential Algebraic Equations index 2 (DAE-2). To solve them numerically, a DAE solver is required. This last representation has the same structure and properties as those reported in (Parra-Vega).

3.3 The robot arm

This section formulates the problem of a manipulator having free mobility on its base. That means, when the base of the robot arm is no longer inertial and thus does not fulfils Newton's laws unless all its dynamic is at new, expressed in a inertial frame.

In order to include the movent of the base of the robot arm, it is necessary to introduce some extra elements which do not appear in the classical fixed-base model. For this case, the free moving base, the inertial frame shall be chosen in the same way it is chosen for the vehicle's: at some point attached to the earth. It is evident that this two references can be identical for the fixed base case, but should certainly be different for the free moving base case. Lets use the inertial reference Σ_0 used for the submarine and define as Σ_b the base frame of the arm when its base is no moving, known as the fixed-base condition.

As a result there are two new homogeneous transformations in the kinematic chain: $H_0^v(q_v)$ from inertial frame Σ_0 to the vehicle's frame Σ_v and H_v^b from Σ_v to the fixed-base first reference frame Σ_b from which all the modelling is obtained.

The homogeneous transformation from inertial frame Σ_0 to the vehicle frame Σ_v is then given by:

$$H_0^v = \begin{bmatrix} R_0^v(\vartheta_v) & d_v \\ 0 & 1 \end{bmatrix} \tag{20}$$

where d_v is the inertial position of the vehicle and $R_0^v \in SO_3$ represents its orientation. Recall that the generalized coordinates of the vehicle are given in (3).

The homogeneous transformation from Σ_v to Σ_b is then given by:

$$H_v^b = \left[\begin{array}{cc} R_v^b & \boldsymbol{d}_{b/v} \\ 0 & 1 \end{array} \right] \tag{21}$$

where $d_{b/v} \in \Re^3$ is the position vector of b wrt vehicle's frame (expressed in Σ_v) and $R_v^b \in SO_3$ represents the orientation that the arm is attached to the vehicle. With the reasonable assumption that the vehicle is a rigid body, and that the assembling is as well, this transformation is constant.

The forward kinematics of the free-base robot arm is given by the concatenation of the proper homogeneous transformations. For instance, the forward kinematic of the end-effector x_e is given by:

$$H_0^e = H_0^v(q_v)H_v^b H_b^e(q_m) = \left[\begin{array}{cc} R_0^e(q_v, q_m) & d_0^e(q_v, q_m) \\ 0 & 1 \end{array} \right]$$

where $H_b^e(q_m)$ stands for the homogeneous transformation of the manipulator , and q_m are the generalized coordinates of the arm chain, both under the fixed-base conditions.

From here on, it is evident that the generalized coordinates for the free-base manipulator shall be extended to include the vehicle configuration as

$$q \stackrel{\triangle}{=} \left(\begin{array}{c} q_v \\ q_m \end{array} \right) \in \Re^{6+n} \tag{22}$$

An acceptable interpretation is that the vehicle is an extra link in the manipulator's chain that has a six degree-of-freedom articulation.

The forward kinematics of the end-effector are given by:

$$d_e = f(q) \;\; = \;\; d_v + R_0^v(\vartheta_v)\left(r_{e/v}^{(v)}(q_m) \right) \tag{23}$$

$$= d_v + R_0^v(\vartheta_v)\left(r_{b/v}^{(v)} + R_v^b d_{e/b}^{(b)}(q_m) \right) \tag{24}$$

where $d_{e/b}^{(b)}(q_m) \in \Re^3$ is the forward kinematic equation on the the fixed-base condition, and $r_{e/v}^{(v)}$ is the position vector of the end-effector from the origin of the vehicle's frame, expressed in that same frame Σ_v.

From eqs. (23)-(24) the linear inertial velocity of the end-effector is:

$$\dot{d}_e = \dot{d}_v + \omega_v \times R_0^v(\vartheta_v)r_{e/v}^{(v)}(q_m) + R_0^v(\vartheta_v)R_v^b \dot{d}_{e/b}^{(b)}(q_m) \tag{25}$$

The linear velocity $\dot{d}_{e/b}^{(b)}(q_m)$ is the fixed-based condition's linear velocity of the end-effector and can be calculated via the linear velocity jacobian: $v_e = J_{vel_{fb}}(q_m)\dot{q}_m$. Then last relationship can also be expressed as

$$\dot{d}_e = \dot{d}_v - \left(R_0^v(\vartheta_v)r_{e/v}^{(v)}(q_m) \right) \times \omega_v + R_0^v(\vartheta_v)J_{vel_{fb}}(q_m)\dot{q}_m \tag{26}$$

The angular velocity of the end-effector is the sum of the vehicle's angular velocity ω_v plus the relative angular velocity of the end-effector respect to the base $\omega_{e/b}$ expressed in the inertial frame. Then, the angular velocity of the end-effector is:

$$\omega_e = \omega_v + R_0^b(\vartheta_v)J_{\omega_{fb}}(q_m)\dot{q}_m \tag{27}$$

where $J_{\omega_{fb}}$ is the angular velocity jacobian for the fixed-base condition. By replacing equation (4) in equations (26) and (27), the end-effector velocity wrench can be written as a function of the extended generalized coordinates and its time derivative as:

$$\nu_{e0} \stackrel{\triangle}{=} \nu_e^{(0)} = \begin{pmatrix} \dot{d}_e \\ \omega_e \end{pmatrix} = \begin{pmatrix} \dot{d}_v - \left[\left(R_0^v(\vartheta_v)r_{e/v}^{(v)}(q_m)\right) \times\right]J_\theta(\vartheta_v)\dot{\vartheta}_v + R_0^b(\vartheta_v)J_{vel_{fb}}(q_m)\dot{q}_m \\ J_\theta(\vartheta_v)\dot{\vartheta}_v + R_0^b(\vartheta_v)J_{\omega_{fb}}(q_m)\dot{q}_m \end{pmatrix} \tag{28}$$

Last equation can also be written in block matrices in the next way:

$$
\begin{aligned}
\nu_{e0} &= \begin{bmatrix} I_3 & -\left[\left(R_0^v(\vartheta_v)r_{e/v}^{(v)}(q_m)\right)\times\right]J_\theta(\vartheta_v) & R_0^b(\vartheta_v)J_{vel_{fb}}(q_m) \\ 0 & J_\theta(\vartheta_v) & R_0^b(\vartheta_v)J_{\omega_{fb}}(q_m) \end{bmatrix} \begin{pmatrix} \dot{d}_v \\ \dot{\vartheta}_v \\ \dot{q}_m \end{pmatrix} \tag{29} \\
&= J_v(q)\dot{q}_v + J_m(q)\dot{q}_m \tag{30} \\
&= J\dot{q} \tag{31}
\end{aligned}
$$

where the *vehicle Jacobian* $J_v \in \Re^{6\times6}$ is defined as:

$$J_v(q) \stackrel{\triangle}{=} \begin{bmatrix} I_3 & -[R_0^v(\vartheta_v)r_{e/v}^{(v)}(q_m)\times]J_\theta(\vartheta_v) \\ 0 & J_\theta(\vartheta_v) \end{bmatrix} \tag{32}$$

and the *manipulator Jacobian* $J_m \in \Re^{6\times n}$ is defined as:

$$J_m(q) \stackrel{\triangle}{=} J_{R_b}(\vartheta_v)J_{fb}(q_m) \tag{33}$$

In the above definitions, the term $[a\times]$ stands for the skew symmetric matrix representation of the cross product of a vector (Spong & Vidyasagar), $J_{R_b} \in SO_6$ is defined as (6) and J_{fb} is the manipulator fixed-base geometric Jacobian. The geometric version of the vehicle Jacobian $J_{v_g}(\vartheta_v, q_m)$ and the manipulator Jacobian $J_m(\vartheta_v, q_m)$ make up the Mobile Manipulator Jacobian defined in (Hootsman & Dubowsky). However, in this work we prefer to use this geometric jacobian because it maps the generalized velocities $\dot{q}$ in linear an angular velocities at any point in the vehicle/ manipulator system.

$$J = \begin{bmatrix} J_v(\vartheta_v, q_m) & J_m(\vartheta_v, q_m) \end{bmatrix} \in \Re^{6\times(6+n)} \tag{34}$$

The dynamics of the free base manipulator can be obtained using the expressions of the kinetic and potential energy of any mass, and using expressions (23) and (29). Because the

generalized coordinates vector has a $6 + n$ dimension, there must be an inertia matrix $\bar{H}$ (q) of the size $(6 + n) \times (6 + n)$ and the vector of generalized forces τ should also have a $6 + n$ dimension.

The kinetic energy of a free-base manipulator is given by:

$$K_m = \sum_{i=0}^{n} \frac{1}{2}\left(\dot{r}_{ci}^T (m_i)\dot{r}_{ci} + \omega_i^T R^i(p) I_i R^{i^T}(p)\omega_i\right) \tag{35}$$

$$= \frac{1}{2}\dot{q}^T \bar{H}(q)\dot{q} \tag{36}$$

where the body 0 is the base, that has no movement in the fixed-base conditions. The linear velocity $\dot{d}_{ci}$ and ω_i are given by equations (26) and (27), respectively, but calculating the distance to the center of mass of the corresponding link.

The resulting solution for this extended inertia matrix can be written as follows:

$$\bar{H}(q) = \left[\begin{array}{cc} M_m(q_v, q_m) & H_A(q_v, q_m) \\ H_A^T(q_v, q_m) & H_{fb}(q_m) \end{array}\right] = \bar{H}^T(q) > 0 \tag{37}$$

which by definition is symmetric and definite positive.

$$M_m \triangleq \left[\begin{array}{cc} \left(\sum_{i=0}^n m_i\right) I_3 & -\sum_{i=0}^n \left(m_i [d_{ci/v}^{(0)}(q)\times]\right) \\ \sum_{i=0}^n \left(m_i [d_{ci/v}^{(0)}(q)\times]\right) & \sum_{i=0}^n \left(R_0^b(R_b^i I_i R_b^{i^T})R_0^{b^T} - m_i [d_{ci/v}^{(0)}(q)\times]^2\right) \end{array}\right] \in \Re^{6\times 6} \tag{38}$$

$$H_A \triangleq \left[\begin{array}{c} R_0^b(q_v)\sum_{i=1}^n m_i J_{vel_{fb_{ci}}}(q_m) \\ \sum_{i=0}^n \left(m_i [d_{ci/v}^{(0)}] R_0^b(q_v) J_{vel_{fb_{ci}}}(q_m) + R^0 (R_0^i I_i R_0^{i^T}) J_{\omega_{bf_i}}\right) \end{array}\right] \in \Re^{6\times n} \tag{39}$$

$$H_{fb} \triangleq \sum_{i=1}^n \left(m_i J_{vel_{fb_{ci}}}(q_m)^T J_{vel_{fb_{ci}}}(q_m) + J_{\omega_{bf_i}}{}^T R_0^i I_i R_0^{i^T} J_{\omega_{fb_i}}\right) \in \Re^{n\times n} \tag{40}$$

Note that Matrix H_{fb} is the inertial matrix of the same robot arm for the fixed-base condition and it depends only in the manipulator coordinates q_m.

On the other hand, being the potential energy, gravitational and buoyant is also function of the vehicle positions, it can be written as a function of the generalized coordinates:

$$V_m = V_m(q) = V_m(q_v, q_m) \tag{41}$$

Then the dynamic equation can be obtained by solving the Euler-Lagrange equation. The resulting model would be of the form:

$$\bar{H}(q)\ddot{q} + \bar{C}(q, \dot{q})\dot{q} + \bar{g}(q) = \bar{\tau}_q + \bar{\tau}_{hydro} \tag{42}$$

where $\bar{C}(q, \dot{q}) \in \Re^{6+n\times 6+n}$ is the Coriolis matrix which has the same properties that for the fixed-base case (i.e. $\frac{1}{2}\dot{\bar{H}} - \bar{C} = Q$; $Q - Q^T = 0$ always true), $\bar{g}(\bar{q}) = \frac{\partial V_m}{\partial \bar{q}}$ is the

gravitational vector of the manipulator and its influence over the vehicle's coordinates and includes the restoring forces due to the floatability of each link, $\bar{\tau}_q$ is the generalized coordinates force vector, and $\bar{\tau}_{hydro}$ are the generalized forces due to the hydrodynamic effects.

This last term is somehow complicated to determine. However, a good approximation is to compute these forces over each link and to translated them to the generalized coordinates, using the virtual work principle (Spong & Vidyasagar), by means of the Mobile Manipulator Jacobian (34) of the geometric center of each link. The resulting vector shall have the next structure (Olguín Díaz):

$$\bar{\tau}_{hydro} = -\bar{D}_m(\cdot)\dot{q} + \bar{\eta}_m(\dot{q}, \zeta(t), \dot{\zeta}(t))$$

where the damping matrix $\bar{D}_m > 0$ is positive definite, due to the fact that the hydrodynamic effects are dissipative, and the hydrodynamical perturbation forces $\bar{\eta}_m$ becomes null when the current is steady ($\zeta(t) = \dot{\zeta} = 0$). The Damping matrix $\bar{D}_m(\cdot)$ can be also be written in block submatrices as:

$$\bar{D}_m(\cdot) = \left[\begin{array}{cc} D_{vv} & D_{vm} \\ D_{mv} & D_{mm} \end{array} \right]$$

Coriolis, gravitational terms, Hydrodynamic damping and current perturbations are highly nonlinear so it is very common to write then together as the non-linear vector $\bar{h}(q, \dot{q}) = \bar{C}(q, \dot{q})\dot{q} + \bar{g}(q) + \bar{D}_m(\cdot)\dot{q} - \bar{\eta}_m(\dot{q}, \zeta(t), \dot{\zeta}(t))$. Then model (42) can be presented as a function of vehicle's and arm's coordinates q_v and q_m:

$$\left[\begin{array}{cc} M_m(q) & H_A(q) \\ H_A^T(q) & H_{fb}(q_m) \end{array} \right] \left(\begin{array}{c} \ddot{q}_v \\ \ddot{q}_m \end{array} \right) + \left(\begin{array}{c} h_{m/v}(q_v, q_m, \dot{q}_v, \dot{q}_m) \\ h_m(q_v, q_m, \dot{q}_v, \dot{q}_m) \end{array} \right) = \left(\begin{array}{c} \tau_{m/v} \\ \tau_m \end{array} \right) \quad (43)$$

Or else, it can be written as two coupled equations as:

$$M_m(q)\ddot{q}_v + H_A(q)\ddot{q}_m + h_{m/v}(q_v, \dot{q}_v, q_m, \dot{q}_m) = \tau_{m/v} \in \Re^6 \quad (44)$$

$$H_A^T(q)\ddot{q}_v + H_{fb}(q_m)\ddot{q}_m + h_m(q_v, \dot{q}_v, q_m, \dot{q}_m) = \tau_q \in \Re^n \quad (45)$$

3.4 The submarine AUV+Robot Arm=SRA

The interaction between the models of the vehicle and the free-base manipulator are forces-torques at the attaching point. So if the original assumption where this attachment is rigid, i.e. it does not nave elastic deformation behaviour, this force wrench shall appeared in both models with opposite direction (due to Newton's 3rd law).

On one hand, this interaction wrench is given in the vehicle dynamics as an external perturbation wrench. This can be seen in the dynamic equation (8) as follows:

$$M_q(q_v)\ddot{q}_v + h_q(q_v, \dot{q}_v) = u_{q_v} + \tau_{arm} \quad (46)$$

where $h_q(q_v, \dot{q}_v) = C_q(q_v, \dot{q}_v)\dot{q}_v + D_q(\cdot)\dot{q}_v + g_q(q_v)) - \eta_q(\dot{q}_v, \zeta(t), \dot{\zeta}(t))$ is the non-linear vector term and τ_{arm} is the perturbation produced by the manipulators movements interaction.

On the other hand, the interaction between the vehicle and the arm, *seen* from the manipulator is the component $\tau_{m/v}$ on either model (43) or (44). By Newton's 3_{rd} law it can be seen that the force wrench $\tau_{m/v}$ on the manipulator model is the same but with opposite direction of the perturbation τ_{arm} on the vehicle's model.

$$\tau_{m/v} = -\tau_{arm} \tag{47}$$

Then by using last equality, a single expression for both model (44) and (46) is found to be:

$$\left[M_q(q_v) + M_m(q_v, q_m) \right] \ddot{q}_v + H_A(q_v, q_m)\ddot{q}_m + h_q(q_v, \dot{q}_v) + h_{m/v}(q_v, \dot{q}_v, q_m, \dot{q}_m) = u_{q_v} \tag{48}$$

Then equations (45) and (48) can be represented by a single whole-system differential equation in a compact form by a coupled pair of differential equations:

$$H(q)\ddot{q} + C(q, \dot{q})\dot{q} + D(\cdot)\dot{q} + g(q) = \tau + \eta(\dot{q}, \zeta(t), \dot{\zeta}(t)) \tag{49}$$

where the nonlinear terms can also be written in a compact form as $h(q, \dot{q}) = C(q, \dot{q})\dot{q} + D(\cdot)\dot{q} + g(q) - \eta(\dot{q}, \zeta(t), \dot{\zeta}(t))$ and the overall terms are given by the next set of relationships [6]:

$$H(q) = \begin{bmatrix} M_v(q_v) + M_m(q_v, q_m) & H_A(q_v, q_m) \\ H_A^T(q_v, q_m) & H_{fb}(q_m) \end{bmatrix} \in \Re^{6+n \times 6+n} \tag{50}$$

$$C(q, \dot{q}) = \begin{bmatrix} C_q(q_v, \dot{q}_v) + C_{vv}(q_v, q_m, \dot{q}_v, \dot{q}_m) & C_{vm}(q_v, q_m, \dot{q}_v, \dot{q}_m) \\ C_{mv}(q_v, q_m, \dot{q}_v, \dot{q}_m) & C_{mm}(q_v, q_m, \dot{q}_v, \dot{q}_m) \end{bmatrix} \tag{51}$$

$$D(\dot{q}, \zeta(t), \dot{\zeta}(t)) = \begin{bmatrix} D_q(\dot{q}_v, \zeta(t), \dot{\zeta}(t)) + D_{vv}(\dot{q}_v, \dot{q}_m, \zeta(t), \dot{\zeta}(t)) & D_{vm}(\dot{q}_v, \dot{q}_m, \zeta(t), \dot{\zeta}(t)) \\ D_{mv}(\dot{q}_v, \dot{q}_m, \zeta(t), \dot{\zeta}(t)) & D_{mm}(\dot{q}_v, \dot{q}_m, \zeta(t), \dot{\zeta}(t)) \end{bmatrix} \tag{52}$$

$$g(q) = \begin{pmatrix} g_q(q_v) + g_{m/v}(q_v, q_m) \\ g_m(q_v, q_m) \end{pmatrix} \tag{53}$$

$$\tau = \begin{pmatrix} u_{q_v} \\ u_{q_m} \end{pmatrix} \in \Re^{6+n} \tag{54}$$

$$\eta(\dot{q}, \zeta(t), \dot{\zeta}(t)) = \begin{pmatrix} \eta_q(\dot{q}_v, \zeta(t), \dot{\zeta}(t)) + \eta_{m/v}(\dot{q}_v, \dot{q}_m, \zeta(t), \dot{\zeta}(t)) \\ \eta_m(\dot{q}_v, \dot{q}_m, \zeta(t), \dot{\zeta}(t)) \end{pmatrix} \tag{55}$$

As well as inthe case of the AUV alone, whenever $\zeta(t) = \dot{\zeta}(t) = 0$, then $)(\cdot) = 0$, and the dynamic equation (49) has the form of a Lagrangian system. Thus, its components fulfills all properties of such systems i.e. definite positiveness of inertia and damping matrices, skew symmetry of Coriolis matrix and appropriate bound of all components.

3.5 SRA in contact
When the end-effector of the SRA gets in contact with the environment, external forces and torques appear in the dynamics that was not taken into account when the dynamics

equations was obtained. Let $F_e = \left(f_e^T, n_e^T\right)^T \in \Re^6$ express the force wrench due to contact forces and torques at the end-effector. From the virtual work principle, this contact force F_e will modify the dynamics of the system through the transpose of the Mobile-Manipulator-Jacobian given by equation (34) as

$$\tau_c = J^T F_e = \left[\begin{array}{c} J_v^T \\ J_m^T \end{array} \right] F_e \tag{56}$$

Which means that the contact forces are translated to the vehicle coordinates by the vehicle's Jacobian and to the joints by the manipulator's Jacobian.

Then equation (49) is modified by adding τ_c as an external force to the righthand side yielding to

$$H(q)\ddot{q} + h(q, \dot{q}) = \tau + J^T F_e \tag{57}$$

In this work, this contact force is also modelled in the same manner as treated in section 3.2, as

$$\tau_c = J^T F_e = J_\varphi^T(q)\lambda \tag{58}$$

Where the $J_\varphi(q)=J_{\varphi+}(q)J(q)$ is the jacobian of the holonomic restriction and λ is the magnitude of the contact force.

4. Open-loop error equation

The introduction of a so called Orthogonalization Principle has been a key in solving, in a wide sense, the force control problem of a robot manipulators with fix base. This physical-based principle states that the orthogonal projection of contact torques and joint generalized velocities are complementary, and thus its dot product is zero, carrying no power and no work is done. Relying on this fundamental observation, passivity arises from torque input to generalized velocities, in open-loop. To preserve passivity in closed-loop, then, the closed-loop system must satisfy the passivity inequality for a given error velocity function. This is true for robot manipulators with fixed frame, and here we extend this approach for robots whose reference frame is not inertial, like SRA. Additionally, we present here the developments that this holds true also for redundant SRA.

4.1 Orthogonalization principle and linear parametrization

Similar to (Liu et al.), the orthogonal projection of $J_\varphi(q)$, which arises onto the tangent space at the contact point, is given by the following operator

$$Q(q) \equiv I_n - J_\varphi^\dagger(q)J_\varphi(q) \in \Re^{(6+n)\text{x}(6+n)} \tag{59}$$

where $I_{6+n} \in \Re^{(6+n)\text{x}(6+n)}$ is the identity matrix and $J_\varphi^\dagger(q) = J_\varphi^T(q)(J_\varphi(q)J_\varphi^T(q))^{-1}$, which always exists since rank$\{J_\varphi(q)\}$ = r. Notice that $rank\left\{Q(q)\right\} = (6+n)-r$ and $Q\dot{q} = \dot{q}$, then $Q(q)J_\varphi^\dagger(q)$=0. Therefore, according to the Orthogonalization Principle, the integral of $(\tau, \dot{q})$ is upper bounded by $-\mathcal{H}(t_0)$, for $\mathcal{H}(t)$ = K + P whenever $\eta(q,\dot{q},\zeta(t),\dot{\zeta}(t)) = 0$ because $\dot{q}^T J_\varphi^t(q)\lambda = 0$

Then passivity arise for the full constrained SRA, under no fluid disturbances. This conclusion gives a very useful and promising theoretical framework, similar to the approach of passivity-based control for fix-base robot arms. On the other hand, it is known that the dynamic equation (49) with no fluid perturbation can be linearly parameterized as follows

$$H(q)\ddot{q} + C(q,\dot{q})\dot{q} + D(\cdot)\dot{q} + g(q) = Y(q,\dot{q},\ddot{q})\Theta, \qquad (60)$$

where the regressor $Y(q,\dot{q},\ddot{q}) \in \Re^{n \times p}$ is composed of known nonlinear functions and $\Theta \in \Re^p$ by p unknown but constant parameters. This is useful to obtain the fundamental change of coordinates of the SRA into the controlled error system, the system expressed in error coordinates, wherein we want to control the system in the trivial equilibria.

4.2 Change of coordinates
In order to design the controller, we need to work out the open loop error equation using (60), in terms of nominal references $\dot{q}_r$, as follows. Consider

$$H(q)\ddot{q}_r + [C(q,\dot{q}) + D(\cdot)]\dot{q}_r + g(q) = Y_r(q,\dot{q},\dot{q}_r,\ddot{q}_r)\Theta, \qquad (61)$$

where $\ddot{q}_r$ is the time derivative of $\dot{q}_r$, *to be defined*. Then the open loop (49) can be written by adding and subtracting (61) as

$$H(q)\dot{s} = -[C(q,\dot{q}) + D(\cdot)]s - Y_r(q,\dot{q},\dot{q}_r,\ddot{q}_r)\Theta + J_\varphi^T(q)\lambda + u_q, \qquad (62)$$

where $s \equiv \dot{q} - \dot{q}_r$ is called the extended error. The problem of designing a controller for the open loop error equation (62) is to find u_q such that $s(*)$ exponentially converges when $Y_r\Theta$ is not available.

4.3 Kinematic redundancy
Notice that

$$X = f(q) \rightarrow \dot{X} = J(q)\dot{q} \qquad (63)$$

Since dimensions of $X \in \Re^m$ and q are not the same, jacobian $J(q) \in \Re^{m \times (6+n)}$, then its inverse does not exists, then to obtain the inverse mapping of (63), we use the pseudoinverse of Penrouse to get

$$\dot{q} = J^\dagger \dot{X} + Q_k v \qquad (64)$$

where matrix $Q_k = (I_{6+n} - J^+(q)J(q)) \in \Re^{(6+n) \times (6+n)}$ stands for the orthogonal projection of $J(q)$ and spans the $6 + n - m$ kernel of $J(q)$, that is $J(q)$ and Q_k are orthogonal complements and its dot product is zero. Now, let consider that Q_k maps any arbitrary vector $v \in \Re^{(6+n)}$ into the null space of $J(q)$. Consider, let

$$\dot{z} = Q_k v \qquad (65)$$

be a vector which belongs to the null space of $J(q)$. This vector yields

$$\dot{z} = Q_k \dot{z} \tag{66}$$

which means that (64) can be written as

$$\dot{q} = J^{\dagger}\dot{X} + \dot{z} \tag{67}$$

That is, given m values of X, we can complete the remaining $6 + n - m$ values of $q \in \Re^{6+n}$ by designing $\dot{z}$ under a given criteria.

4.4 Orthogonal nominal reference

Since $\dot{q} = Q\dot{q}$, and considering the decomposition (67) to design the extended error $s = \dot{q} - \dot{q}_r \equiv Q\dot{q} - \dot{q}_r$, and aiming at preserving passivity in closed loop, it is natural to consider a structure for $\dot{q}_r$ similar to $\dot{q}$, that is the nominal reference $\dot{q}_r$ at the velocity level takes de following form

$$\dot{q}_r = Q\left(J^{\dagger}\dot{X}_r + \dot{z}_r\right) + \beta J_{\varphi}^T\left(s_F - s_{dF} + \gamma_2\int_{t_0}^t sgn\{s_{qF}(t)\}dt\right), \tag{68}$$

with

$$\dot{X}_r = \dot{X}_d - \sigma\tilde{X} + s_{dp} - \gamma_1\int_{t_0}^t sgn\{s_{qp}(t)\}dt \tag{69}$$

where $\tilde{X} \triangleq X(t) - X_d(t)$, $X_d(t)$ and $\lambda_d(t)$ are the desired smooth trajectories of position and contact force $\tilde{\lambda} \triangleq \lambda(t) - \lambda_d(t)$ as the position and force tracking errors, respectively. Parameters β, σ, γ_1 and γ_2 are constant matrices of appropriate dimensions; and $sgn(y)$ stands for the entrywise signum function of vector y, and

$$s_p = \dot{\tilde{X}} + \sigma\tilde{X}, \tag{70}$$

$$s_{dp} = s_p(t_0)e^{-\alpha(t-t_0)}, \tag{71}$$

$$s_{qp} = s_p - s_{dp}, \tag{72}$$

$$s_{vp} = s_{qp} + \gamma_1\int sgn(s_{qp}(\varsigma))d\varsigma, \tag{73}$$

$$s_F = \int_{t_0}^t \tilde{\lambda}dt, \tag{74}$$

$$s_{dF} = s_F(t_0)e^{-\eta(t-t0)}, \tag{75}$$

$$s_{qF} = s_F - s_{dF}, \tag{76}$$

$$s_{vF} = s_{qF} + \gamma_2\int sgn(s_{qF}(\varsigma))d\varsigma \tag{77}$$

for $\alpha > 0$, $\eta > 0$. Finally, the reference for $\dot{z}$, that is $\dot{z}_r$ introduces a reconfigurable error, such that tracking errors in the null space will also converge to its desired value and full control on the redundancy is introduced. To this end, consider

$$\dot{z}_r = \dot{z}_d - \alpha_z \Delta z + s_{dz} - \gamma_z \int \operatorname{sgn}(s_{qz}) \tag{78}$$

where $\dot{z}_r$ fulfills $Q_k \dot{z}_r = \dot{z}_r$ in such a way that

$$s_z = \Delta \dot{z} + \alpha_z \Delta z = (\dot{z} - \dot{z}_d) + \alpha_z(z - z_d) \tag{79}$$

$$s_{dz} = \beta_z s_z(t_0) e^{-\kappa t} \tag{80}$$

$$s_{qz} = s_z - s_{dz} \tag{81}$$

$$s_{vz} = s_{qz} + \gamma_z \int \operatorname{sgn}(s_{qz}) \tag{82}$$

for positive definite feedback gains $\alpha_z, \beta_z, \gamma_z$. To complete the definitions, consider

$$\dot{z}_d = Q_k v_d \tag{83}$$

where $v_d = k \frac{\partial}{\partial q} \Omega$ stands for the gradient of a given cost function Ω to be optimized. According to this cost function, the redundant degrees of freedom of the full open kinematic chain tracks $\dot{z}_d$ and z_d, as it will be proved in the following, where

$$z_d = \int \dot{z}_d + z_d(t_0) \tag{84}$$

for without loss of generality it is assumed that $z_d(t_0) = q(t_0)$. Finally, owing to the fact that $\dot{q} = Q(J^\dagger \dot{X} + \dot{z})$ and that $s_r = \dot{q} - \dot{q}_r$, we obtain then

$$s = Q\left\{J^\dagger(\dot{X} - \dot{X}_r) + (\dot{z} - \dot{z}_r)\right\} - \beta J_\varphi^T s_{vf} \tag{85}$$

$$= Q\left\{J^\dagger s_{vp} + s_{vz}\right\} - \beta J_\varphi^T s_{vf} \tag{86}$$

where s_{vp}, s_{vF}, and s_{vz} respectively, are given by (73), (77) and (82). Notice that $J^\dagger s_{vp}$ and s_{vz} are orthogonal complements $(J^\dagger s_{vp})^T s_{vz} = 0$ and so does $Q(*)$ and J_φ^T. Notice that although the time derivative of $\dot{q}_r$ is discontinuous, that is not of any concern because it is not used in the controller.

5. Model-free second order sliding mode controller

Consider the following nominal continuous control law:

$$u_q = -K_d s + J_{\varphi+}^T(q)\left(-\lambda_d + \dot{s}_{dF} + \gamma_2 \tanh(\mu s_{qF}) + \mu s_{vF}\right) \tag{87}$$

with $\mu > 0$ and $K_d = K_d^T > 0, \in \Re^{(6+n)\text{x}(6+n)}$. This nominal control, designed in the q-space can be mapped to the original coordinates of the vehicle model, expressed by the set (1)-(2), using the next relationship $u_v = J_\nu^{-T}(q)u_{q_v}$. Thus, the physical controller in the vehicle u_v is implemented in terms of a key inverse mapping J_ν^{-T}.

5.1 Closed-loop system
The open loop system (62) under the continuous model-free second order sliding mode control (87) yields to

$$H\dot{s} = -[C + D + K_d]s - Y_r\Theta + J_{\varphi+}^T(\dot{s}_{vF} + \eta s_{vF}) + \gamma_2 J_\varphi^T Z + \tau^* \tag{88}$$

where $Z = tanh(\mu s_{qF}) - sgn(s_{qF})$, and $\tau^* \equiv 0$ is useful for the passivity analysis.

5.2 Stability analysis
Theorem Consider a constrained SRA (57)under the continuous model-free second order sliding mode control (87). The Underwater system yields a second order sliding mode regime with local exponential convergence for the position, and force tracking errors.
Proof. A passivity analysis $\langle S, \tau^* \rangle$indicates that the following candidate Lyapunov function V qualifies as a Lyapunov function

$$V = \frac{1}{2}(s^T H s + \beta s_{vF}^T s_{vF}), \tag{89}$$

for a scalar $\beta > 0$. The time derivative of the Lyapunov candidate equation immediately leads to

$$\begin{aligned}
\dot{V} &= -s^T(K_d + D_q)s - \beta\eta s_{vF}^T s_{vF} - s^T Y_r\Theta + s^T\gamma_2 J_\varphi^T Z \\
&\leq -s^T K_d s - \beta\eta s_{vF}^T s_{vF} + \|s\|\|Y_r\Theta\| + \|s\|\|\gamma_2\|\|J_\varphi\|\|Z\| \\
&\leq -s^T K_d s - \beta\eta s_{vF}^T s_{vF} + \|s\|\|\epsilon\|,
\end{aligned} \tag{90}$$

where it has been used the skew symmetric property of $\dot{H} - 2C(q, \dot{q})$, the boundedness of both the feedback gains and submarine dynamic equation (there exists upper bounds for $H, C(q, \dot{q}), g(q), \dot{q}_r, \ddot{q}_r$), the smoothness of $\varphi(q)$ (so there exists upper bounds for J_φ and $Q(q)$), and finally the boundedness of Z. All these arguments establish the existence of the functional ϵ. Then, if K_d, β and η are large enough such that s converges into a neighborhood defined by ϵ centered in the equilibrium $s = 0$, namely as $t \rightarrow \infty$, one obtains

$$s \rightarrow \epsilon \tag{91}$$

This result stands for local stability of s provided that the state is near the desired trajectories for any initial condition. This boundedness in the $\mathcal{L}_\infty$ sense, leads to the existence of the constants $\epsilon_3 > 0$, $\epsilon_4 > 0$ and $\epsilon_5 > 0$ such that

$$\|\dot{s}_{vp}\|_{\mathcal{L}_\infty} < \epsilon_3, \tag{92}$$

$$\|\dot{s}_{vz}\|_{\mathcal{L}_\infty} < \epsilon_4, \tag{93}$$

$$\|\dot{s}_{vF}\|_{\mathcal{L}_\infty} < \epsilon_5. \tag{94}$$

An sketch of the local convergence of s_{vp} is as follows[1]. Boundedness of **s** means boundedness of the projected vectors $Q_k s_z$ and $J^\dagger(q)s_{vp}$, then if we multiply them we get zero, then we can analyze independently each projected vector. Locally, in the $n - r$ dimensional image of Q, we have that $s_{vp}^* = Q s_{vp} \in \Re^n$. Consider now that under an abuse of notation that $s_{vp} = s_{vp}^*$, such that for small initial conditions, if we multiply the derivative of s_{vp} in (73) by s_{qp}^T, we obtain

$$s_{qp}^T \dot{s}_{qp} = -\gamma_1 |s_{qp}| + s_{qp}^T \dot{s}_{vp} \le -\gamma_1 |s_{qp}| + |s_{qp}||\dot{s}_{vp}| \le -(\gamma_1 - \varepsilon_3)|s_{qp}| \tag{95}$$

which have used (92), and $\gamma_1 > \epsilon_3$, to guarantee the existence of a sliding mode at $s_{qp}(t) = 0$ at time $t \le \|s_{qp}(t_0)\|/(\gamma_1 - \epsilon_3)$, and according to the definition of s_{qp} (72), $s_{qp}(t_0) = 0$, which simply means that $s_{qp}(t) = 0$ for all time.

Similar than for s_{vp}, if we multiply the derivative of s_{vz} in (79) by s_{qz}^T, we obtain

$$s_{qz}^T \dot{s}_{qz} = -\gamma_z |s_{qz}| + s_{qz}^T \dot{s}_{vz} \le -\gamma_z |s_{qz}| + |s_{qz}||\dot{s}_{vz}| \le -(\gamma_z - \varepsilon_5)|s_{qz}| \tag{96}$$

which have used (93), and $\gamma_z > \epsilon_4$, to guarantee the existence of a sliding mode at $s_{qz}(t) = 0$ at time $t \le \|s_{qz}(t_0)\|/(\gamma_z - \epsilon_4)$, and according to the definition of s_{qz} in (79)-(82), $s_{qz}(t_0) = 0$, which simply means that $s_{qz}(t) = 0$ for all time.

Finally, we see that if we multiply the derivative of (77) by s_{vf}^T, we obtain

$$s_{qF}^T \dot{s}_{qF} = -\gamma_2 |s_{qF}| + s_{qF}^T \dot{s}_{vF} \le -\gamma_2 |s_{qF}| + |s_{qF}||\dot{s}_{vF}| \le -(\gamma_2 - \varepsilon_4)|s_{qF}| \tag{97}$$

which have used (94), and $\gamma_2 > \epsilon_5$, to guarantee the existence of a sliding mode at $s_{qp}(t) = 0$ at time $t \le \|s_{qF}(t_0)\|/(\gamma_2 - \epsilon_5)$ and, according to (77), $s_{qF}(t_0) = 0$, which simply means that $s_{qf}(t) = 0$ for all time, which simply implies that $\lambda \to \lambda_d$ exponentially fast.

6. Simulation results

Simulations has been made on a simplified and idealized platform of a 6 dof submarine with a mass of 100 kg, where the floatability point it is assumed to be in the geometrical centre of the vehicle. It is also assumed that the vehicle has neutral floatability i.e. the buoyancy forces equals the gravity ones. The submarine vehicle was modeled as a regular cube, so its principal moments of inertia are represented by a constant diagonal matrix. In order to get a simple but reliant dynamic model, we considered the base of the robot arm to be in the geometrical center of the vehicle. This robot arm was based on the 6 DoF Mitsubishi PA-10 with a mass of 30 kg. We also assumed that the spherical wrist only contributes in orientation, that is, the last link has length zero. The robot arm principal moments of inertia are as well assumed to be diagonal matrices.

---

[1] The strict analysis follows (*Liu, et. al.*)

Now even when our simulator is simple, it contains most of the coupled dynamics from the vehicle and the robot arm, which still makes the control problem quite a challenge.

Simulations were realized using the simulation software 20Sim 4.0, on a 64-bit Windows Vista computer with 4 GB RAM memory at 2.1 GHz Dual-Core processor. Simulator presents tridimensional results (x, y, z, roll, pitch, yaw), so the generalized coordinates for the vehicle is given by:

$$q_v = \begin{pmatrix} x_v & y_v & z_v & \phi_v & \theta_v & \psi_v \end{pmatrix}^T \tag{98}$$

which represents the cartesian position and orientation of the vehicle. The generalized coordinate for the robot arm is given by:

$$q_m = \begin{pmatrix} q_1 & q_2 & q_3 & q_4 & q_5 & q_6 \end{pmatrix}^T \tag{99}$$

which represents the manipulator joint positions. The generalized coordinates for the SRA system is composed by the vehicle and robot arm generalized coordinates, and is given by:

$$q = \begin{pmatrix} q_v \\ q_m \end{pmatrix} \tag{100}$$

The holonomic constraint is given by a vertical surface located at 1 meter from the origin, who's expression is

$$\varphi(q) \equiv x - 1 = 0 \tag{101}$$

It is assumed that the SRA end-effector remains in contact with the environment for all the time. In order to satisfy the constraint equation, the initial conditions were chosen as:

$$q_v(t_0) = \begin{pmatrix} 0 & 0 & 0 & 0 & 0 & 0 \end{pmatrix}^T \tag{102}$$

$$q_m(t_0) = \begin{pmatrix} 0 & 0 & -\pi/2 & 0 & -\pi/4 & 0 \end{pmatrix}^T \tag{103}$$

which leads to the following end-effector initial pose:

$$X(t_0) = \begin{pmatrix} 1 & 0 & 1 & 0 & -3\pi/4 & 0 \end{pmatrix}^T \tag{104}$$

Now, the desired end effector position and orientation trajectory task are defined as:

$$X_d = \begin{pmatrix} x_d & y_d & z_d & \phi_d & \theta_d & \psi_d \end{pmatrix}^T \tag{105}$$

$$X_d = \begin{pmatrix} 1 & 1 - \cos(t/10) & 0.9 + 0.1\cos(t/2) & 0 & 3\pi/4 & 0 \end{pmatrix}^T \tag{106}$$

On the other hand, the desired force profile applied by the SRA end effector on the contact surface (holonomic constraint) is represented by:

$$\lambda_d = 20\sin(t/2) + 100 \tag{107}$$

The model-free control parameters are as follows:

q_i	K_d	γ_1	σ	α	β	μ
x_v	400	10^{-3}	9	20	1	100
y_v	400	10^{-3}	9	20	1	100
z_v	400	10^{-3}	9	20	1	100
ϕ_v	400	50^{-3}	9	20	1	100
θ_v	400	50^{-3}	9	20	1	100
ψ_v	400	50^{-3}	9	20	1	100
q_1	80	80^{-3}	22	70	5	100
q_2	110	80^{-3}	22	70	5	100
q_3	100	80^{-3}	18	70	5	100
q_4	28	50^{-3}	5	70	5	100
q_5	25	50^{-3}	5	70	5	100
q_6	20	50^{-3}	4	70	5	100

And the force scalar gains were defined as $\eta = 2$, $\gamma_2 = 10^{-1}$.

6.1 Numerical considerations

To compute the value of λ, the constrained Lagrangian that fulfils the constrained movement, can be calculated using the second derivative of the holonomic restriction: $\ddot{\varphi}(q) = 0$. Then, by using the dynamic equation (49) and after some algebra its expression becomes either:

$$\lambda = \left[J_\varphi H^{-1} J_\varphi^T \right]^{-1} \left(J_\varphi H^{-1} \left(h(q, \dot{q}, t) - u_q \right) - \dot{J}_\varphi \dot{q} \right) \tag{108}$$

The set of eqns. (49)-(108) describes the constrained motion of the SRA when in contact to infinitely rigid surface described by (12). Numerical solutions of these sets can be obtained by simulation, however the numerical solution, using a DAE solver, can take too much effort to converge due to the fact that these sets of equation represent a highly stiff system. In order to minimize this numerical drawback, the holonomic constraint has been treated as a numerically compliant surface which dynamic is represented by

$$\ddot{\varphi}(q) + D\dot{\varphi}(q) + P\varphi(q) = 0. \tag{109}$$

This is known in the force control literature of robot manipulators as constrained stabilization method, which bounds the nonlinear numerical error of integration of the backward integration differentiation formula. With a appropriate choice of parameters P and D, the solution of $\varphi(, t) \to 0$ is bounded. This dynamic is chosen to be fast enough to allow the numerical method to work properly. In this way, it is allowed very small deviation on the computation of λ, typically in the order of -10^6 or less, which may produce, according to some experimental comparison, less than 0.001% numerical error. Then, the value of the normal contact force magnitude becomes:

$$\lambda = \left[J_\varphi H^{-1} J_\varphi^T \right]^{-1} \left(J_\varphi H^{-1} \big(h_v(q, \dot{q}, t) - u_q \big) \dot{J}_\varphi \dot{q} - D J_\varphi \dot{q} - P \varphi(q) \right), \qquad (110)$$
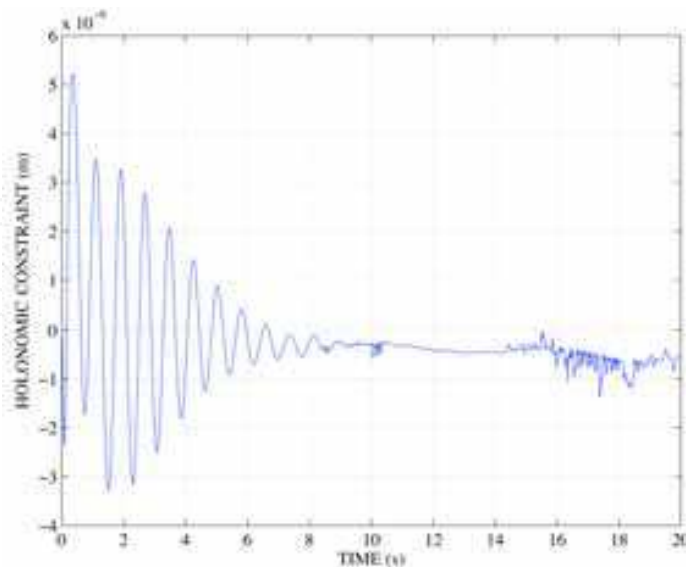

Figure 1. Holonomic constraint using the constraint stabilizer

6.2 Model free position-force tracking control

Figure 2 shows the end-effector's cartesian position. It is important to remark that the end-effector $x = 1$ position, correspond to the holonomic constraint, which is asumued to be satisfied for all the time, that because of the infinitely rigid object assumption given in in (12). On the other hand, the y, z positions are the desired end effector trajectories over the contact surface. Note that all the end effector positions are given in the inertial frame.
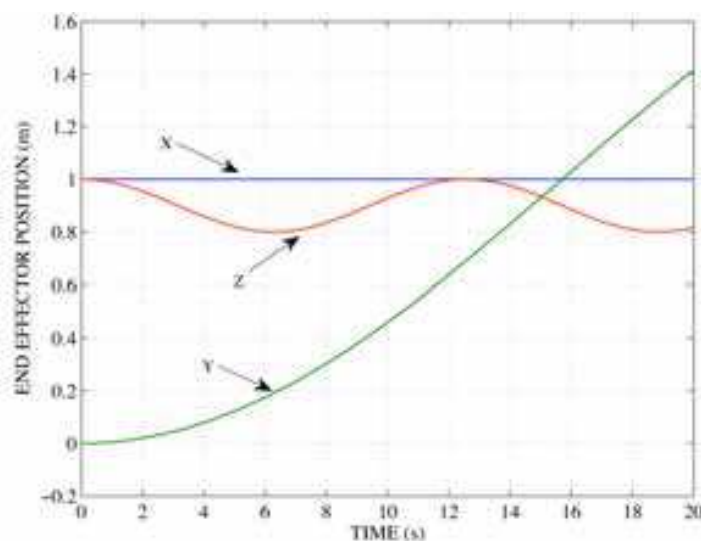
Figure 2. End-effector tracking desired position y, z while remaining in contact with the holonomic constraint all the time.

On Figure 3 we find the end-effector orientation angles, which were defined as the roll-pitch-yaw angles around the x-y-z axis of the inertial frame. It can be seen that orientation tracks a desired orientation with all angles at at constant values of 0 for the roll and yaw angles, and $3\pi/4$ for the pitch angle.
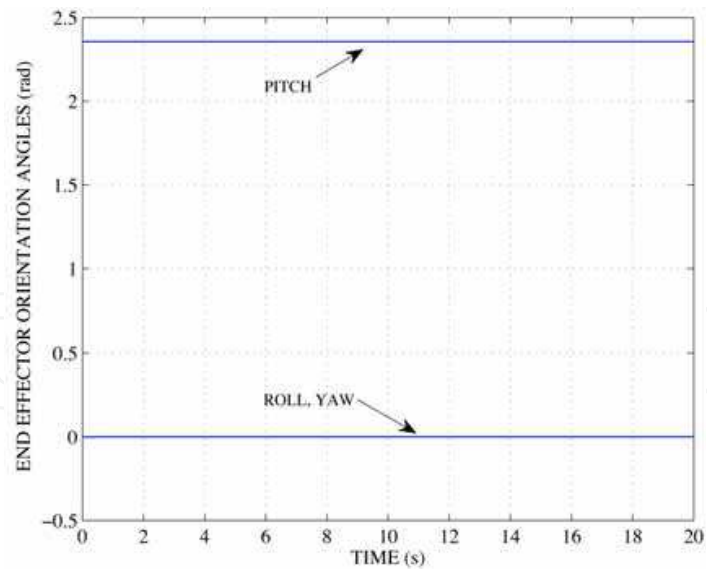
Figure 3. End-effector's orientation angles (roll, pitch, yaw), where we can see that set-point tracking tasks on 0 and 3π/4 rad are being performed by the system.

Figure 4 shows how the end effector linear velocity vector evolves over time. In this Figure, we can observe that x velocity remains on 0, while the y and z velocities tracks 1/10cos(t/10) and 0.05cos(t/2) respectively. This way, both set-point control and tracking are being performed by the system.
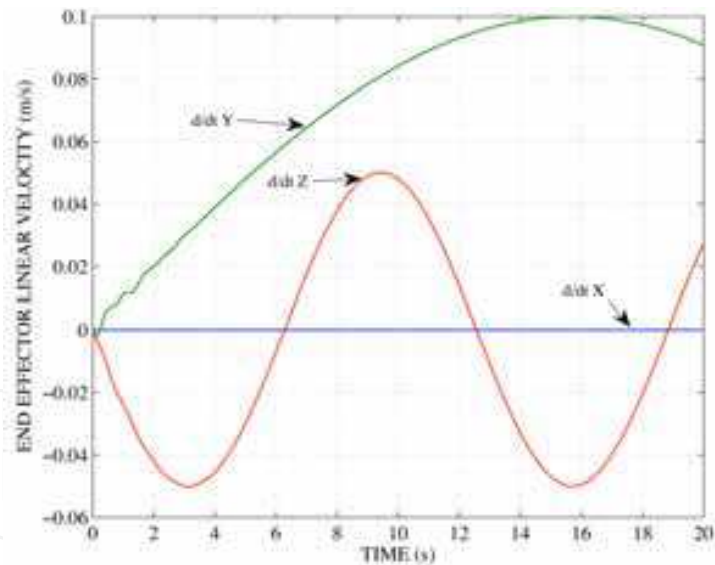
Figure 4. End-effector linear x-y-z velocities, where both, regulation and tracking are performed

Given the parameters used to describe the end-effector orientation, Figure 5 shows the time derivative of these orientation parameters, which in the strictly mathematical sense, are different form the end-effector angular velocity. In this figure, we can see that the orientation derivative, after a small transient finally establish at zero radians, that is, the end effector orientation will remain in the same position for all the time.

Now, let us define X as the 6 dof end-effector pose (position and orientation) vector, and $\tilde{X} = X - X_d$ as the pose error vector. Figure 6 shows the Euclidean norm of the end effector

pose error ($\|\tilde{X}\|$) and the norm of the end effector analytic velocity error ($\|\dot{\tilde{X}}\|$), which must not be confused with the geometric velocity error. In this figure, it is very clear that the error manifold are nearly zero, because of the controller inner properties.
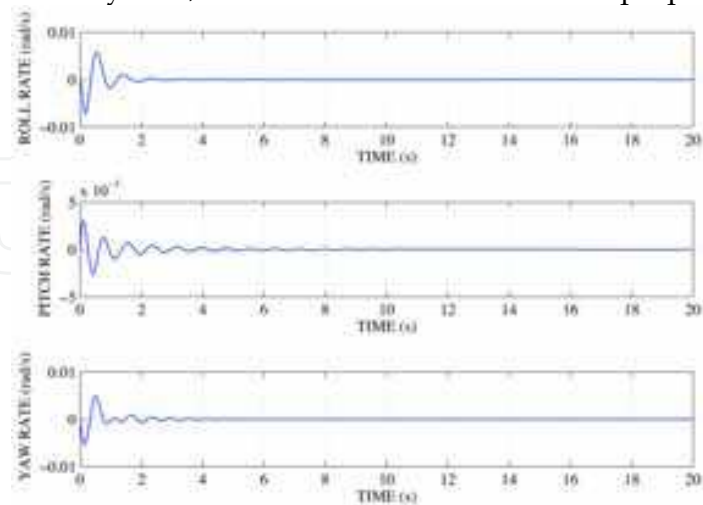
Figure 5. End-effector variation of angle parameters ($\dot{\phi}, \dot{\theta}, \dot{\psi}$) converge to zero after a small transient
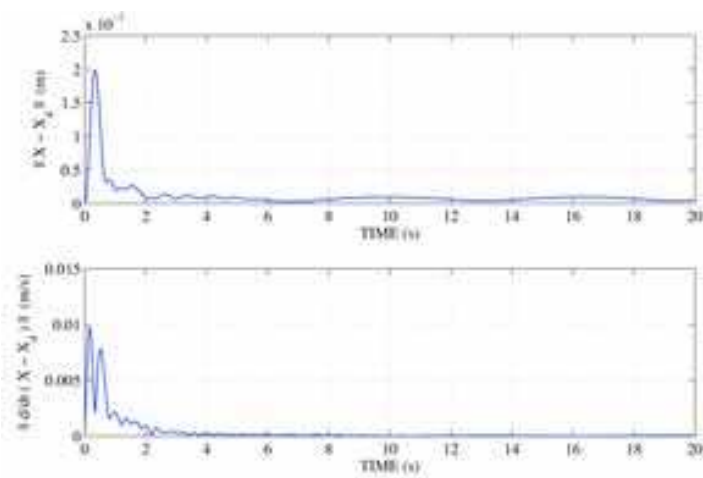
Figure 6. Euclidian norms of the end-effector's pose and its time derivative ($\tilde{X}$, $\dot{\tilde{X}}$), where it is very clear the stability properties of the controller

Similarly as with the position, we defined a force task which must be accomplished by the end effector when moving around the contact surface. This task is independent from the position one, in other words, we can control both position and force simultaneous and independently. Figure 7 presents the end-effector force tracking trajectory (λ), where a periodic signal mounted on an offset of 100 N is shown. Additionally, Figure 7 shows on the right upper frame, a zoom of how the contact force, tracks the desired force profile. On the right lower frame, we can see the norm of the contact force error which is defined as $\|\tilde{\lambda}\| = \|\lambda - \lambda_d\|$. This error shows how fast the controller makes the contact force to track, with very little error, the desired contact force trajectory.

In relation with the control signals, Figure 8 shows the x-y-z linear forces applied to the vehicle. On this set of figures we can observe that no linear forces present chattering. This

characteristic is very representative of the second order sliding mode controllers. Note that the biggest control signal belongs to the x linear force, this because of the shared contribution of the vehicle and the manipulator to achieved the contact force on the holonomic constraint, positioned along the x axis.
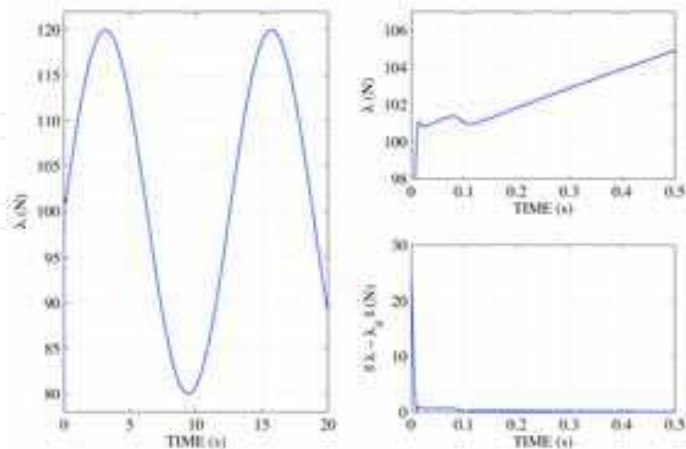
Figure 7. Left frame shows the end-effector contact force trajectory (λ), right upper frame shows a zoom of this force, and the right lower frame shows the norm of the end effector contact force $|| \tilde{\lambda} ||$
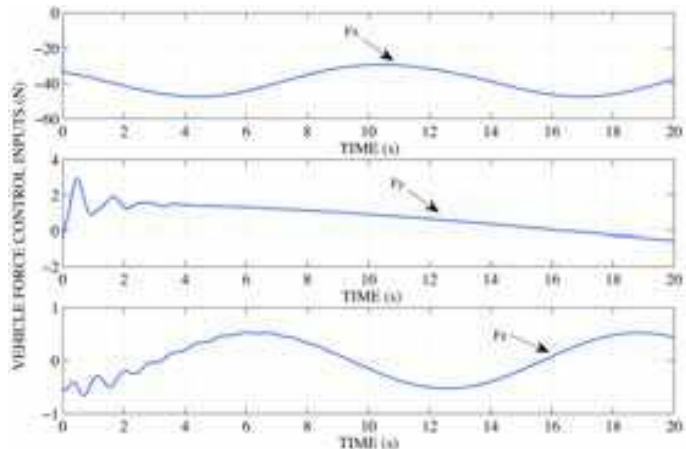
Figure 8. The x-y-z linear inertial forces applied to the vehicle, where the contact force contribution is mainly made through the x linear force

The vehicle torque control inputs can be seen in Figure 9, where, just as in the linear force case, no chattering is present on the signals. In this figure, we can see that x and z torque inputs are nearly cero, contrary to the y torque input, whose value oscillates around -30 Nm. due to the torque created by the distance of the contact point to the vehicle's origin.

Likewise, Figure 10 shows the torques (τ_i) applied to the robot arm joints, where torque inputs τ_4, τ_5, τ_6 are nearly cero, this is because these three joints only contribute on the end effector orientation in other words, the final link connected to them has length zero. Note that joint torque 2 are the one that mostly contribute to the end effector contact force.

Now, Figures 11-14 show the generalized coordinates sliding surfaces, that is, the vehicle and manipulator generalized coordinates surfaces. On these figures it can been shown that the error manifolds converge to a stable bounded neighborhood centered in the origin. We

know that even when actual modern actuators have been growing really fast in past few year, it is still imposible to implement a signum function on them, that is the main reason why a saturation function is preferred. With the use of this saturation function we may no get ideal results, instead we get this convergence region where error stabilize.
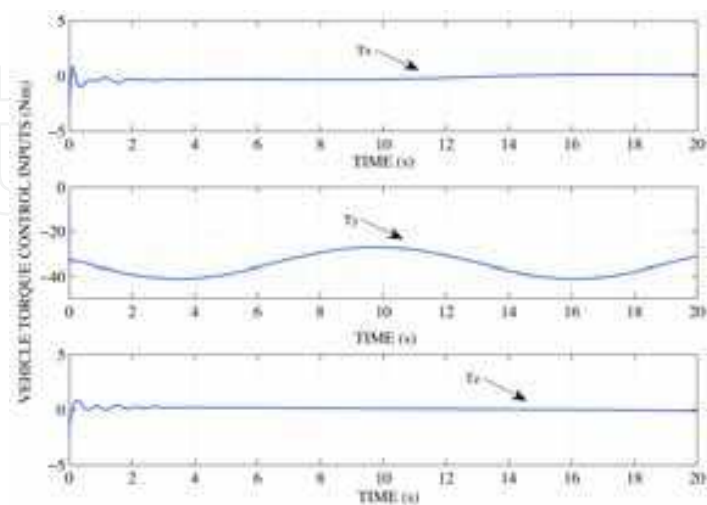

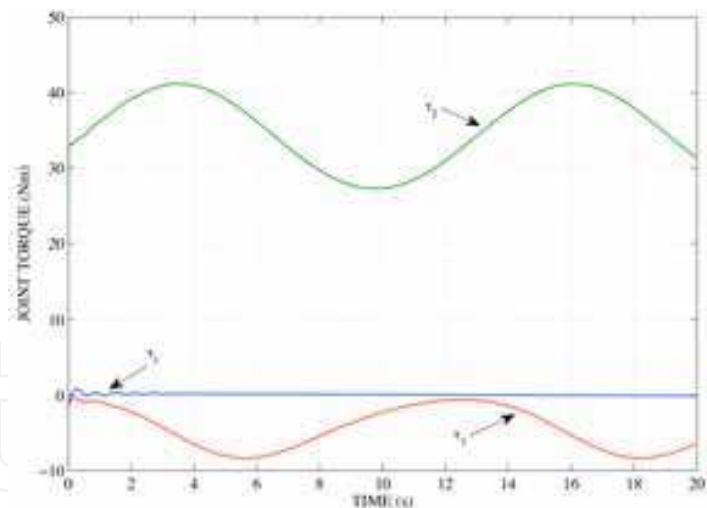Figure 9. Input torques (n_x, n_y, n_z) applied to the vehicle, where we can see that n_x and n_z are nearly cero

Figure 10. Input control torques (τ_i) applied to the robot-arm, where the contact force contribution is mainly made through joint 2

On the other hand, Figure 15 shows the force error manifold, on which can be seen that the force error converge to a stable bounded neighborhood centered in the origin. It is very clear that this force manifold is the strongest one on the controller.

In consequence of the highly redundancy of the submarine robot arm (12 dof) working in normal operational conditions (6 dof), some degrees of freedom can be used to perform an additional task like minimize energy consumption, maximize dexterity, maximize the

distance to the mechanical limits, etc. These additional tasks can be made by projecting a vector into the null space of the jacobian matrix.

Using the very know result of the gradient descendent, we can locally optimize a performance criteria like the ones already mentioned.
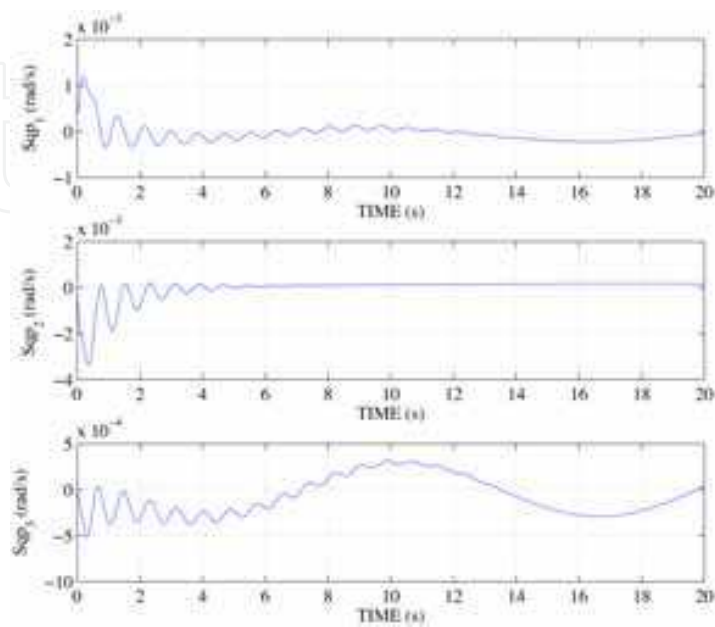
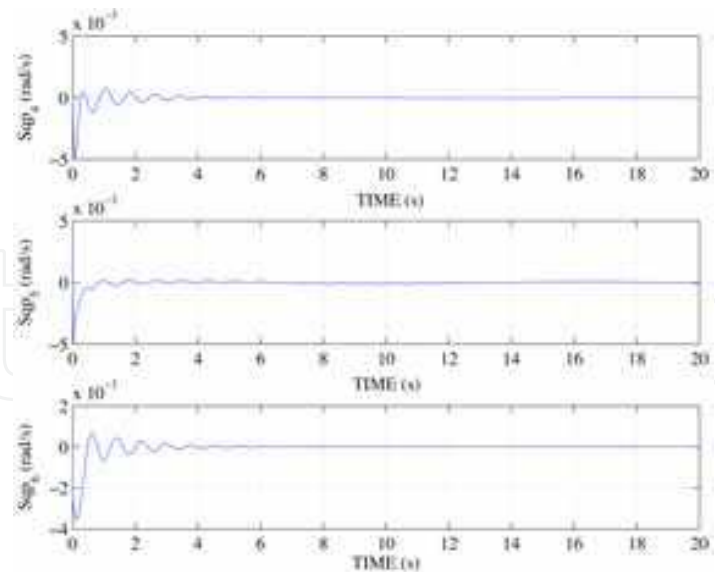Figure 11. Generalized coordinates 1-3 position sliding surface

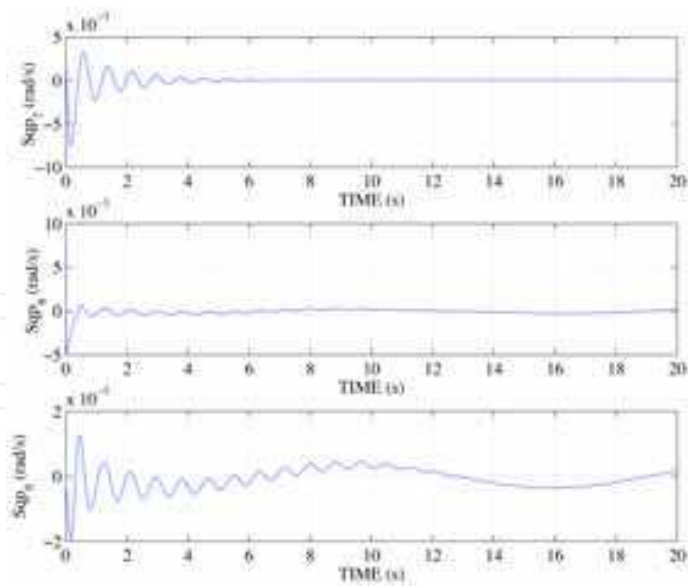Figure 12. Generalized coordinates 4-6 position sliding surface

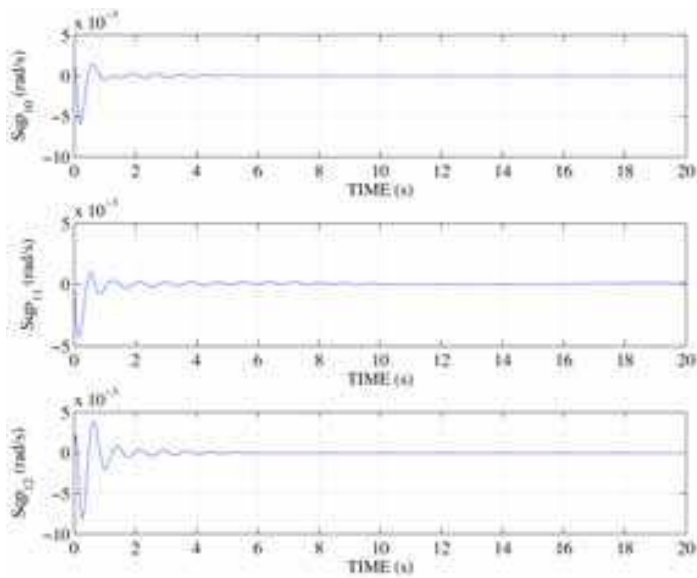Figure 13. Generalized coordinates 7-9 position sliding surface

Figure 14. Generalized coordinates 10-12 position sliding surface

Simulations results are presented using the distance to the mechanical limits as the performance criteria, this criteria is given by:

$$\omega = \frac{1}{2n} \sum_{i=1}^{n} \left(\frac{q_i - \bar{q}_i}{q_{iM} - \bar{q}_{im}} \right)^2 \tag{111}$$

where $q_{iM}(q_{im})$ represents the maximum (minimum) limit for the generalized coordinate q_i, and $\bar{q}_i$ is the medium point for a coordinate range.

Figure 16 shows the performance criteria locally optimized for the required position-force trajectory, where curve lower minima represents a local optimal configuration.
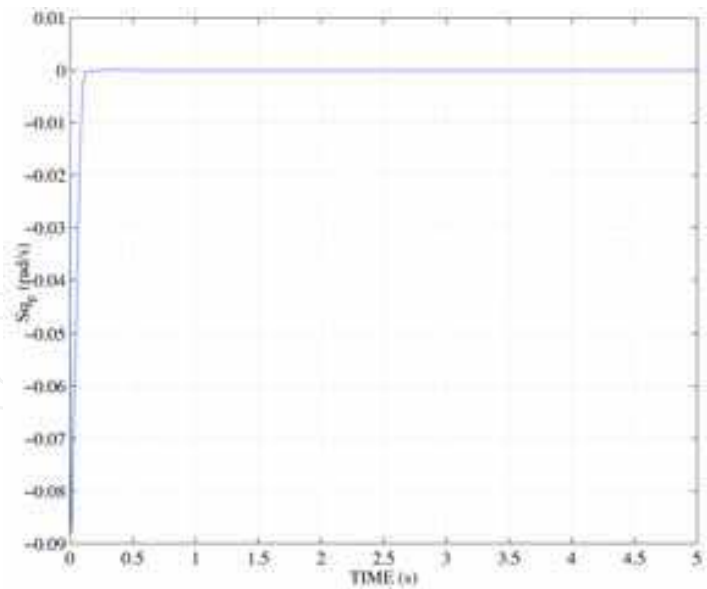
Figure 15. Force sliding surface

7. Remarks

There are several discussions that arise in such a complex system. In particular the dynamic model deserves further discussions related to its structural properties. Also, the simple control structure highlights its simplicity in contrast to the complex dynamics. Friction at the contact point is another issue we did not include. Finally redundancy is an additional structural degree of freedom which could be used to successfully tackle security issues too.
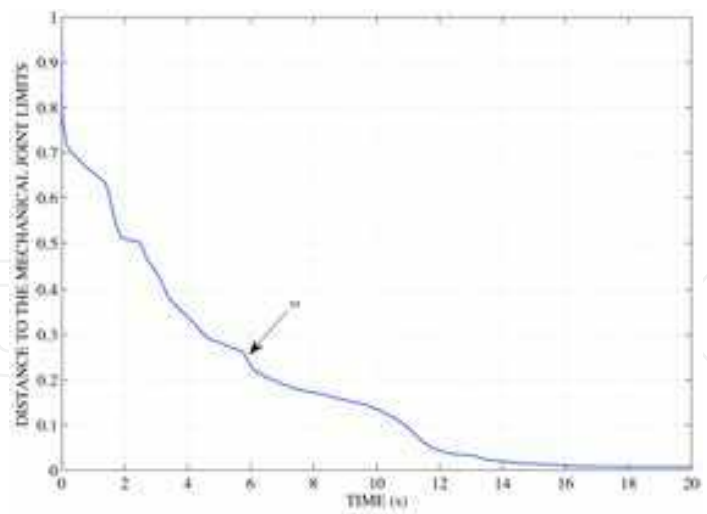

Figure 16. Redundancy resolution performance criteria (ω)

Properties of the Dynamics As it was pointed out in section 3, the model of a submarine robot can be expressed in either a *self space* where the inertia matrix is constant for some conditions that in practice are not difficult to met or in a generalized coordinate space in which the inertial matrix is no longer constant but the model is expressed by only one

equation likewise the kinematic lagrangian chains. Both representations preserves the all well-known properties of lagrangian systems such skew symmetry for the Coriolis/Inertia matrix, boundedness of all the components and passivity preserved properties for the hydrodynamics added effects, including buoyancy.

Properties of the Kinematics In this way, the kinematic equation gives rise to an equivalence of these representations. The latter is a linear operator that maps generalized coordinates time derivative with a generalized physical velocity. This relationship is specially important due to the fact that time derivative of angular representations (such a roll-pitch-yaw) is not the angular velocity, however there is always a correspondence between these vectors. For external forces this mapping is indeed important. It relates a physical force/torque wrench to the generalized coordinates $q = (x_v, y_v, z_v, \phi_v, \theta_v, \psi_v)$ whose last 3 components does not represent a unique physical space. In this work such mapping is given by J_v and appears in the contact force mapping by the either the mobile manipulator Jacobian $J(q)$ or the holonomic restriction Jacobian J_φ.

The Controller Although a PD controller, recently validated by (Smallwood & Whitcomb 2004), has a much simpler structure and acceptable performance for underwater vehicles in position control schemes, it does not deal with the task of contact force control. Notice that the controller exhibits a PD structure plus a nonlinear I-tame control action, with nonlinear time-varying feedback gains, for each orthogonal subspace. It is in fact a decentralized PID-like, called "Sliding PD" controller, with two inner control loops and two kernels, one for contact point, where generalized velocities arise, and one for the self motion, evolving in the kernel of the observable output. It is indeed surprising that similar control structures can be implemented seemingly for a robot in the surface or below water, with similar stability properties, attaining simultaneous tracking of contact force and posture. Of course, this is possible under a proper mapping of Jacobians, key to implement this controller.

Friction at the contact point When friction at the contact point arises, which is expected to submarine tasks wherein the contact object is expected to exhibits a rough surface, with high friction coefficients, a tangential friction model should be added in the right hand side. Particular care must be placed to map the generalized velocities. Since this forces are nonconservative, it is expected, under proper handling of these dissipative forces in the error coordinates system, that stability will be enhanced.

8. Conclusions

Structural properties of the open-loop dynamics of submarine robots are key to design passivity-based controllers. In this paper, an advanced, yet simple, controller is proposed to achieve simultaneously tracking of time-varying contact force and posture, without any knowledge of the dynamics of the SRA. This is a significant feature of this controller, since in particular for submarine robots the dynamics are very difficult to compute, let alone its parameters. The redundancy is resolved at the kernel of the generalized velocities, such as primary, typically tracking errors, and secondary tasks can be satisfied. A simulation study of a hyper-redundant SRA provides additional insight into the closed-loop dynamic properties for set-point control and tracking case. It is proved that redundancy introduces a level of dexterity previously unexposed for SRA, while achieving critical contact force control.

9. References

E. Olguín-Díaz, V. Parra-Vega *On the Force/Posture Control of a Constrained Submarine Robot* 4th International Conference on Informatics in Control, Robotics and Automation, Conference Prodeedings. May 2007

Smallwood, D.A.; Whitcomb, L.L. *Model-based dynamic positioning of underwater robotic vehicles: theory and experiment* Oceanic Engineering, IEEE Journal of Volume: 29 Issue: 1 Jan. 2004

V. Parra-Vega, Second Order Sliding Mode Control for Robot Arms with Time Base Generators for Finitetime Tracking, Dynamics and Control, 2001.

Smallwood, D.A.; Whitcomb, L.L. *Toward model based dynamic positioning of underwater robotic vehicles* OCEANS, 2001. MTS/IEEE Conference and Exhibition Volume: 2 2001

Villani, L.; Natale, C.; Siciliano, B.; Canudas de Wit, C.; *An experimental study of adaptive force/position control algorithms for an industrial robot* Control Systems Technology, IEEE Transactions on Volume 8, Issue 5, Sept. 2000

E. Olguín-Díaz, *Modélisation et Commande d'un Système Véhicule/Manipulateur Sous-Marin* PhD Thesis. Laboratoire d'Automatique de Grenoble, January 1999

Y. H. Liu, S. Arimoto, V. Parra-Vega, and K. Kitagaki, *Decentralized Adaptive Control Of Multiple Manipulators in Cooperations*, International Journal of Control, Vol. 67, No. 5, pp. 649-673, 1997.

M. Perrier, C. Canudas de Wit, "Experimental Comparison of PID versus PID plus Nonlinear Controller for Subsea Robots" *Journal of Autonomous Robots, Special issue on Autonomous Underwater Robots, 1996.*

V. Parra-Vega and S. Arimoto, *A Passivity-based Adaptive Sliding Mode Position-Force Control for Robot Manipulators*, International Journal of Adaptive Control and Signal Processing, Vol. 10, pp. 365-377, 1996.

Arimoto, *S. Fundamental problems of robot control* Robotica (1995), volume 13, pp 19-27,111-122, Cambrige University Press

Thor I. Fossen. *Guidance and Control of Ocean Vehicles*. John Wiley and Sons, Chichester 1994

I. Schjølberg, T. I. Fossen. "Modelling and Control of Underwater Vehicle-Manipulator Systems" Proceedings the 3rd Conference on Marine Craft Maneuvering and Control (MCMC'94), Southampton, UK, 1994.

Chiaverini, S.; Sciavicco, L. *The parallel approach to force/position control of robotic manipulators*. IEEE Transactions on Robotics and Automation Volume 9, Issue 4, Aug. 1993

IFREMER, Project VORTEX: *Modélisation et simulation du comportement hidrodynamique d'un véhicule sous-marin asservi en position et vitesse.* 1992

Sagatun, S.I.; Fossen, T.I.; *Lagrangian formulation ofunderwater vehicles' dynamics* Decision Aiding for Complex Systems, Conference Proceedings., 1991 IEEE International Conference.

N. Hootsman & S. Dubowsky. Large Motion Control of Mobile Manipulators Including Vehicle Suspension Characteristics *Procedings of the 1991 IEEE International Conference on Robotics and Automation. Sacramento, California. (April 1991)*

Spong M.W., Vidyasagar M. *Robot dynamics and control*. John Wiley, New York 1989

Yoerger, D.; Slotine, J. *Robust trajectory control of underwater vehicles* Oceanic Engineering, IEEE Journal of Volume: 10 Issue: 4 Oct 1985

Robotics Automation and Control

Edited by Pavla Pecherkova, Miroslav Flidr and Jindrich Dunik

This book was conceived as a gathering place of new ideas from academia, industry, research and practice in the fields of robotics, automation and control. The aim of the book was to point out interactions among various fields of interests in spite of diversity and narrow specializations which prevail in the current research. The common denominator of all included chapters appears to be a synergy of various specializations. This synergy yields deeper understanding of the treated problems. Each new approach applied to a particular problem can enrich and inspire improvements of already established approaches to the problem.

How to reference

In order to correctly reference this scholarly work, feel free to copy and paste the following:

E. Olguín-Díaz, V. Parra-Vega and D. Navarro-Alarcón (2008). Control of Redundant Submarine Robot Arms under Holonomic Constraints, Robotics Automation and Control, Pavla Pecherkova, Miroslav Flidr and Jindrich Dunik (Ed.), ISBN: 978-953-7619-18-3, InTech, Available from:
http://www.intechopen.com/books/robotics_automation_and_control/control_of_redundant_submarine_robot_arms_under_holonomic_constraints

INTECH
open science | open minds